JOURNAL OF APPLIED ELECTROCHEMISTRY 7 (1977) 277–286

Temperature distribution along the gap in electrochemical machining

W. G. CLARK, J. A. MCGEOUGH

Department of Engineering, University of Aberdeen, Marischal College, Aberdeen, UK

Received 23 October 1975; and in revised form 16 February 1977

The temperature of the flowing electrolyte solution within the inter-electrode gap has been measured by means of miniature bead-thermistors. For NaCl solution the temperatures recorded within the gap are higher than those outwith the gap. As the flow-rate is reduced the temperature within the gap increases to a maximum which corresponds closely to the boiling state of the electrolyte. These results are consistent with measurements in a region of increased resistivity within the gap such as that provided by the hydrogen bubble–electrolyte layer adjacent to the cathode. Similar tests with $NaNO_3$ solution have shown that the temperatures within the gap are much lower with that electrolyte than with NaCl solution. These effects follow previous observations that substantially less hydrogen gas is evolved with $NaNO_3$ than with the NaCl electrolyte.

Notation

b electrode breadth
c_e specific heat of electrolyte
e^* non-dimensional quantity $\left(=\dfrac{e_a - e_g}{e_a}\right)$
e_a electrochemical equivalent of anode metal
e_g electrochemical equivalent of hydrogen gas
f mechanical feed-rate of anode
h inter-electrode gap width
J current density
L electrode length
Q volumetric flow-rate of electrolyte
T electrolyte temperature
U electrolyte velocity
V applied voltage
x distance along electrode
x^* non-dimensional distance $\left(=\dfrac{\rho_a f x}{\rho_e h_o U_o}\right)$
ΔT temperature rise of electrolyte between inlet and outlet
ΔV sum of overvoltages and reversible potentials (assumed constant)
ρ_a anode density
ρ_e electrolyte density
Subscript o inlet condition

1. Introduction

The temperature variation of the electrolyte solution flowing along the inter-electrode gap has a significant bearing on many aspects of the electrochemical machining (ECM) process. A well-known effect concerns the taper in the width of gap along the electrode length, due partly to the change in electrolyte temperature in the downstream direction of flow. Another is the limit on the rate of machining, which can be imposed by boiling of the electrolyte [1]. Investigations of such effects have been greatly hampered by experimental difficulties in measuring the temperature of the electrolyte within the machining gap. The small width of gap, typically about 0·5 mm, means that the mercury thermometer is impractical, whilst the thermocouple is rendered useless by the action upon its junction of the electric fields present during ECM, and by the rapid disintegration of the junction by the flow. In consequence, measurements of the electrolyte temperature are normally taken outwith the machining gap at nearby stations upstream and downstream from it. The increase in temperature of the electrolyte between these points, arising from electrolyte heating in the gap caused by the passage of current,

is commonly found to follow the theoretical rise predicted from Joule's and Ohm's laws [2]. This relationship is therefore assumed in most analyses of the effects of electrical heating of the electrolyte in the gap, such as the taper in width, mentioned above [3].

In this paper, a technique for measuring the temperature of the electrolyte solution in the inter-electrode gap during ECM is described. The measurements have revealed that the temperature rise of the electrolyte in the gap can be substantially greater than that predicted from Joule's heating theory. These results arise from phenomena occurring within the gap, and cannot be anticipated if the temperature is only read at inlet and outlet points to the machining gap. (Some initial experimental results from this investigation are described in brief elsewhere [1].)

2. Theory

For an electrolyte flowing between plane, parallel electrodes, of breadth b and length L and separated by a gap at inlet of h_o, the temperature rise ΔT between inlet and outlet points to the machining gap is usually assumed, from Joule's and Ohm's laws, to have the simple form [1]:

$$\Delta T = \frac{(V-\Delta V)JbL}{\rho_e c_e Q}. \quad (1)$$

Thorpe and Zerkle have used the same basic assumptions implicit in Equation 1 to predict the variation of the solution temperature $T(x)$ as a function of distance x along the electrode length

$$T(x) - T(o) = \frac{1}{e^*}\left(\frac{V-\Delta V}{e_a c_e}\right)\ln(1+e^*x^*) \quad (2)$$

where $T(o)$ is the electrolyte temperature at the inlet [3]. Now $e^* < 1$ and substitution of typical values shows that $x^* < 1$, so that $e^*x^* < 1$ [1].

Thus the above Equation 2 reduces to

$$T(x) - T(o) = \frac{V-\Delta V}{e_a c_e}\frac{\rho_a f x}{\rho_e h_o U_o}. \quad (3)$$

Now for equilibrium ECM

$$f = \frac{e_a J}{\rho_a} \quad (4)$$

and since $Q = bh_oU_o$, Equation 3 becomes

$$T(x) - T(o) = \left(\frac{V-\Delta V}{c_e\rho_e}\right)\frac{Jbx}{Q}. \quad (5)$$

In the present work, calculations have been based on these values of the appropriate variables: $V = 32\,V$, $\Delta V = 1{\cdot}2\,V$, $J = 16\,A\,cm^{-2}$, $c_e = 3{\cdot}73\,kJ\,(kg\,K)^{-1}$, $b = 12{\cdot}7\,mm$, $L = 100\,mm$, $\rho_e = 1070\,kg\,m^{-3}$. The value for ΔV has been estimated from the reversible potential for iron (0·44 V) and the sum of the activation (Tafel) overpotentials at both electrodes; concentration overpotential has been assumed to be made negligible by the electrolyte flow.

3. Experimental apparatus and procedure

From a review of possible instruments for measuring the temperature of the electrolyte solution in the gap during ECM, the miniature bead-thermistor was identified as a likely device. Its main advantages are that the bead at its tip is made of a thermally-sensitive, semi-conductor material and that the bead is enclosed in a glass envelope. The instrument is thereby protected during ECM from attacks of the type described in the Introduction. Another useful feature is that the thermistor can readily be attached to a recording instrument. 'S.T.C. type FS' thermistors were selected; their bead-diameter is about 1 mm, the smallest commercially available.

The ECM cell for use with rectangular plane, parallel electrodes and designed to house the thermistors, is shown in Fig. 1. It was built mainly from two polypropylene plates which were bolted together, the flow channel for the electrolyte being machined out of one plate. A slot to the dimensions of the electrodes, 100 by 12·7 mm, was also cut through the two plates, into which the mild steel anode and stainless steel cathode could be placed with a press-fit. This procedure, together with sealing at all interfaces by 'o' rings, ensured that the electrolyte flow was completely confined to the gap between the electrodes.

Before the cathode was fitted into the cell, six thermistors, spaced 18 mm apart, were inserted through the electrode so that their tips protruded 0·9 mm from its surface. The thermistors were set in this position with Araldite.

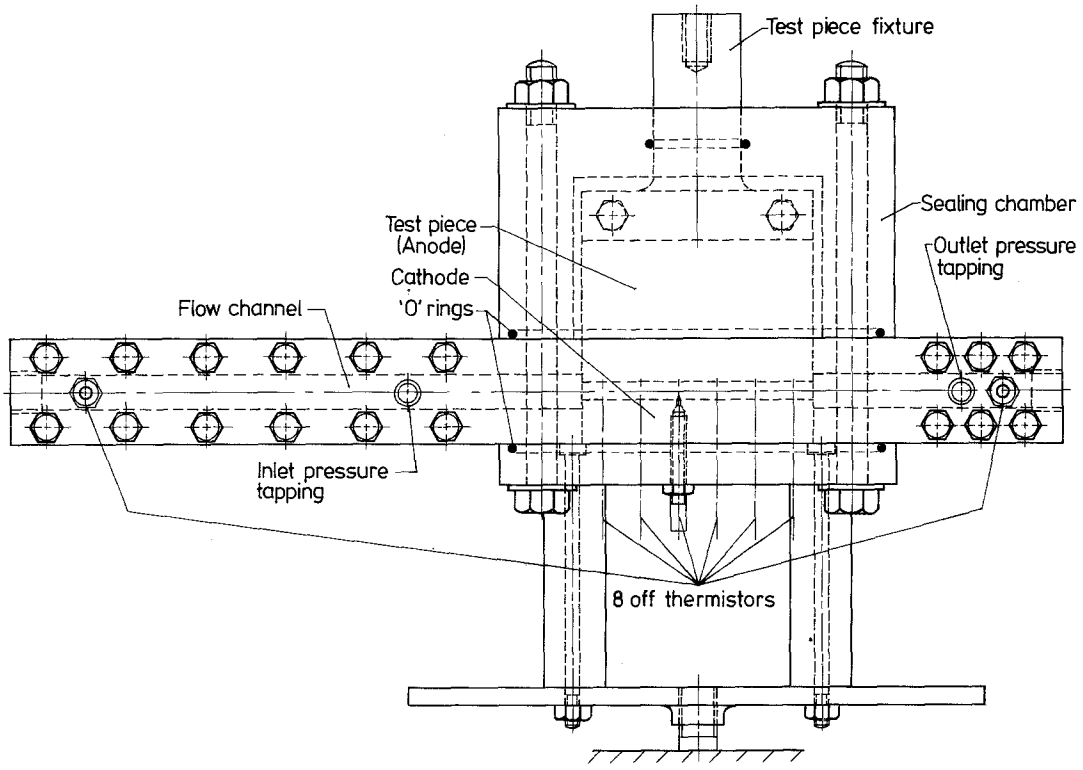

Fig. 1. Main features of ECM cell for measurement of temperature.

The thermistors were calibrated for temperatures up to 100° C by immersing the cathode assembly in a beaker of water placed on a heater–stirrer unit. This unit enabled constant temperatures to be maintained during calibration. For temperatures in the range 95 to 145° C, a light oil was used instead of water. The logarithmic variation of resistance with temperature of the thermistors was then measured with a Wayne Kerr 'Universal Bridge'. The time-response of the thermistors to changes in temperature was also checked by dipping the thermistor fixture into water at various known temperatures. The thermistor resistance changed very rapidly to about 75% of the value corresponding to each temperature, the final value being achieved in less than 10 s. This time compared closely with the response of the thermistors before mounting in the cathode. It was concluded that the proximity of the thermistor tips to the cathode surface therefore had a negligible effect on the measurements.

The cathode carrying the thermistors was then fitted in the cell. Two other calibrated thermistors were inserted into the flow channel at the inlet and at the outlet point, seven hydraulic diameters from the electrodes. The ECM cell itself was mounted on an electrochemical machine which enabled the anode electrode to be driven vertically towards the cathode at rates between 0·1 and 8·0 mm min^{-1}. These feed-rates were determined by means of an impulse tachometer mounted on the spindle of the feed-drive motor; the advance of the anode towards the cathode was measured with a 0·01 mm dial gauge. Power was supplied from a rectifier capable of 250 A at 32 V. The output voltage was stabilized against variation in load current, and measured with a 0–32 V voltmeter. Current was read from a 0–500 A ammeter.

The electrolyte was drawn from a reservoir of capacity 0·25 m^3 by a 'Mono' pump, capable of a pressure of 750 kN m^{-2} and a maximum flow-rate of 30×10^{-5} m^3 s^{-1}, and was delivered through nylon-braided polythene piping to the cell. A by-pass valve fitted to the delivery side of the cell allowed the flow-rate to be varied, whilst the outlet pressure to the pump was controlled by a needle-valve. The electrolyte temperature in the main tank was maintained constant by means of a

heat exchanger operated from a cold water supply. The electrolyte was also filtered to remove particles which might have interfered with the ECM action in the gap. The electrolyte flow-rate was measured with a 'Rotameter' flow-meter, while its pressure at inlet and outlet to the cell was measured with stainless steel Bourdon gauges.

Each anode specimen was first ground so that its face could be aligned parallel to the cathode. After the specimen was fitted into the cell, the initial electrode gap was set by placing a slip, ground to the required size, on the cathode, and by moving the anode forward until contact was made. This position was noted from the dial gauge; then the anode was retracted, the slip removed, and the specimen again brought to the fixed position.

Electrolyte was next pumped through the gap. After the flow became steady, the flow-rate and pressure were adjusted to the required values. In order to check further the reliability of the thermistors, at this stage, the readings on the pen-recorder were compared with the calibrations and with the temperatures given by two thermometers, at inlet to the gap and at the flow discharge point.

The current was then switched on, and the anode drive engaged. As the electrode drive started, the time of machining was taken with a stop-watch. During ECM, the temperature distribution of the electrolyte along the gap was measured with the thermistors, each of which was connected through the multiple switch box to the continuously balanced universal bridge, the output being displayed on a pen-recorder. The scan of all the thermistors could be made in about 2 min; the readings were taken twice during each ECM test, which ran for about 6 to 8 min.

The operating conditions for these experiments had to be selected primarily to ensure sufficient clearance in the electrode gap for the thermistor tips. (It will be recalled that these protruded 0·9 mm into the gap.) For that purpose a voltage of 32 V and a constant feed-rate of 0·35 mm min^{-1} were used. The corresponding gap width at inlet was 2·35 mm, the electrolyte temperature there being 293 K. These conditions yielded a current density of approximately 16 A cm^{-2} with the 10% (w/w) NaCl solution mainly used in this work. (For comparative purposes another NaCl and a 17% $NaNO_3$ electrolyte were used in later tests. Their pertinent data are given at the appropriate parts of the next section.) Electrolyte flow-rates ranging from 2×10^{-5} to 24×10^{-5} m^3 s^{-1} were used; and the pressure at outlet was varied between 101 and 290 kN m^{-2}.

4. Results and discussion

In Fig. 2, the experimental temperature rise for the NaCl solution measured directly between the inlet and outlet points to the machining gap, shows reasonable agreement with the theoretical increase, calculated from Equation 1. However, the temperatures recorded by the thermistor within the gap, 6 mm from outlet, were noted as higher than those measured at the outlet station. As the flow-rate is reduced, the temperature within the gap rises to a maximum, which corresponds closely to the boiling point of the NaCl solution for each outlet pressure. For example, the recorded maximum temperature is about 389 K for the outlet pressure of 170 kN m^{-2} and the flow-rate of $3{\cdot}8 \times 10^{-5}$ m^3 s^{-1}; the corresponding tabulated boiling point of the solution is 391 K [4]. In contrast, at the outlet station, the measured electrolyte temperature is approximately 335 K for the same flow-rate and pressure. Decrease in the flow-rate to $3{\cdot}5 \times 10^{-5}$ m^3 s^{-1} increases the outlet temperature to about 337 K without further effect on the temperature measured within the gap.

A slight variation in the 'boiling point' is particularly noticeable for the 170 kN m^{-2} outlet pressure, although this effect was also encountered at the other pressures. It appeared to coincide with small fluctuations in the flow-rate and outlet pressure, which arose when the flow-rate was reduced below about 5×10^{-5} m^3 s^{-1}. Simultaneously with the onset of these fluctuations, small oscillations occurred in the cell voltage. It is relevant that voltage fluctuations observed previously in ECM have been attributed to the presence of cathodically evolved hydrogen gas [5].

The similar fluctuations encountered in the present work, and the higher temperatures recorded within the gap, also seem to be due to the evolution of hydrogen gas at the cathode. The mixture of electrolyte and hydrogen gas bubbles constitute a region, the resistivity of which is greater than that of a 'pure' electrolyte uncon-

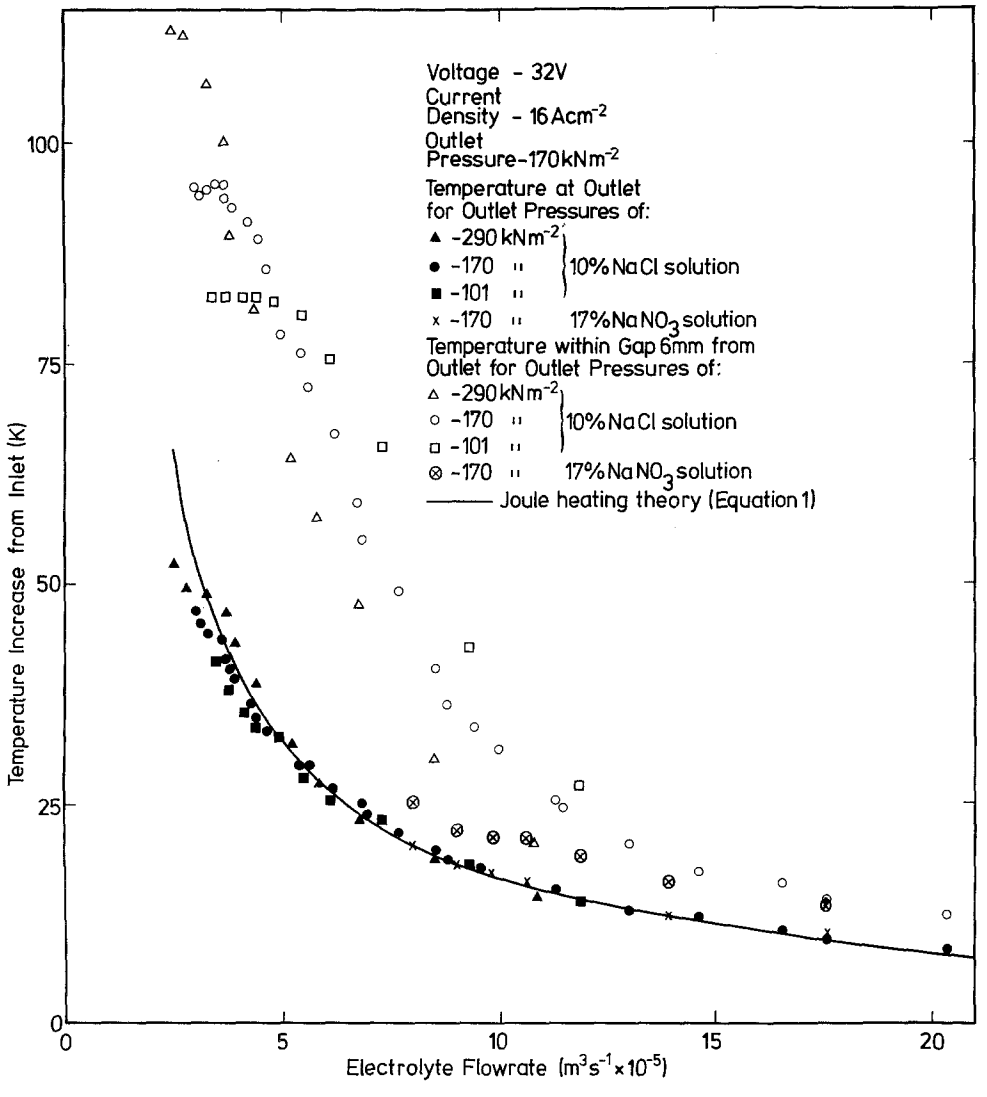

Fig. 2. Variation of temperature increase with flow-rate and outlet pressure.

taminated by hydrogen. The resistive heating, and hence the measured temperature, of the gas–electrolyte mixture will therefore be greater than that of the pure electrolyte.

Although the solution temperature within the gap is known to increase with decreasing flow-rate due to Joule heating, the higher increases observed may also be associated with the well-established observation that the diameter of the hydrogen gas bubbles increases with decreasing electrolyte velocity [5, 6]. Larger bubbles will cause greater resistivity of the mixture, and therefore greater electrical heating. Sufficient decrease in the rate of flow will lead to the maximum possible temperature of the mixture, i.e. its boiling point.

Although the thermistors successfully provided measurements of the temperature of the solution within the machining gap, their presence there would have complicated the pattern of flow. In particular, when the electrolyte met the leading thermistor, a mixing wake would be created on the downstream side of the thermistor bead. The succeeding thermistors, each located in the wake of its predecessor would ensure continued efficient mixing of the solution along their entire line. Since the wake would also spread out from the line of thermistors, a sufficiently wide expansion, aided

by the turbulence of the solution, would thoroughly disperse the hydrogen bubbles throughout the electrolyte. The thermistors would then have disrupted the 'bubble layer' observed photographically by Hopenfeld and Cole [7] and Landolt *et al.* [5] and predicted theoretically by Stronach *et al.* [8].

The temperatures recorded by the thermistors would then be representative of the entire solution within the gap, and not just that of the gas–electrolyte mixture in their neighbourhood. But if the solution had been completely in that state, then, as it flowed out of the machining gap, its temperature would have been unlikely to drop so rapidly to the considerably lower temperature measured by the outlet thermistor, sited seven hydraulic diameters downstream (see Fig. 2). Indeed, from Equation 1 these temperatures are similar to those calculated for a pure electrolyte, uncontaminated by hydrogen bubbles, which would have a lower resistivity.

Although these results are therefore difficult to interpret fully, a better understanding may lie with the work of Loutrel and Cook [9]. They claim that a thin layer of hydrogen bubbles is attached to the cathode surface, as well as an outer bubble layer, which flows with the electrolyte. Landolt *et al.* also report that some bubbles stick to the cathode surface during ECM, while other bubbles become detached (and presumably form the accepted bubble layer).

If the bubbles within the gap do take that formation, then the thermistor beads, sited on the cathode surface, would mainly have recorded the temperature of the inner layer and only partially that of the outer region of gas and electrolyte now thoroughly mixed because of the thermistors. The size of the inner bubbles should still be influenced by electrolyte velocity and pressure [5, 6, 8]. They are, in any case, believed to be larger than those in the outer region [5, 9]. The consequent higher resistivity of the inner layer means a locally higher temperature recorded by the thermistors there.

As the electrolyte flowed out of the machining gap, the abrupt expansion of the flow channel would have caused rapid mixing of the inner hot layer with the outer solution, presumably cooler and of much greater bulk. The outlet thermistor would then have recorded the considerably lower temperature of a solution with the hydrogen gas bubbles now dispersed entirely throughout it. Fig. 2 indicates that the bulk solution must have been sufficiently cool and that the hot inner layer must have been sufficiently absorbed in it to reduce the average temperature to that predicted from Joule heating (Equation 1). It is of interest that Hopenfeld and Cole mention, without explanation, outlet temperatures in excess of those calculated from the simple Joule theory [7]. In their case, the bubbles could not have been mixed sufficiently with the bulk electrolyte at the outlet station. In consequence, the temperature of a locally hotter region would seem to have been measured. Fig. 2 also shows that the higher the pressure at outlet, the lower the temperature within the machining gap recorded by the thermistors. These observations are consistent with a decrease in the size of the hydrogen bubbles with increasing absolute pressure [6], and thus with a correspondingly lower void fraction of the electrolyte–bubble mixture.

The temperatures measured beyond the machining gap are independent of the outlet pressure. This result again suggests that the conditions of flow at outlet render the solution an effectively pure one, unaffected by the hydrogen bubbles.

Equation 5 shows that from the Joule theory the electrolyte temperature should also increase along the gap even for a solution of constant resistivity. The rise calculated from that equation and presented in Fig. 3 is again lower than the observed increase recorded with the thermistors. A contribution to the latter higher temperatures of the bubble–electrolyte solution may likewise come from the cumulative effect of the electrolyte flow along the electrode upon the temperature of the mixture. Additionally, however, progressively more bubbles become gathered in the solution as it moves downstream, so that a corresponding increase in its resistivity should be expected. That is, the gradient of the temperature rise along the electrode should be greater than that caused only by the combined effect of flow and Joule heating: indeed, the condition is confirmed in Fig. 3.

A sufficiently high resistivity of the bubble region will clearly lead to boiling. Fig. 3 provides further evidence for greater resistive heating of the bubble–electrolyte mixture at lower flow-rates in

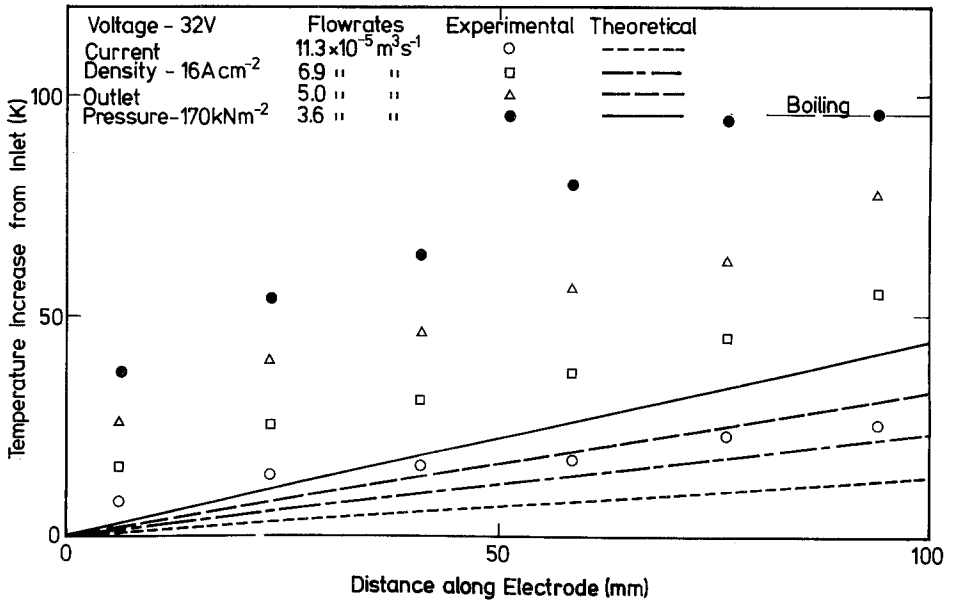

Fig. 3. Temperature increase along electrode length (NaCl solution).

which case the diameter of the hydrogen bubbles is greater. Sufficiently far downstream, boiling then becomes probable, as indicated in Fig. 3 for the lowest flow-rate of $3{\cdot}6 \times 10^{-5}$ m^3 s^{-1}. In the experiments, on further reduction in flow-rate, the onset of boiling could be made to occur further upstream. That observation is consistent with increased resistance heating of the bubble–electrolyte region discussed above.

It should be noted in Fig. 3 that the temperatures registered by the leading thermistors account for a major part of the temperature rise along the electrode length. Stagnation of the electrolyte flow at the leading edge of that thermistor would have created a substantially voided region of gas and electrolyte there. The average temperature recorded by the thermistor for the solution in that condition would then be greater than one which was agitated entirely around the thermistor.

Fig. 4 shows the corresponding variations in the electrode gap width along the electrode length, obtained from measurements of the anode profile. The convention used to specify the variation in gap width is that the gap at inlet, 2·35 mm is taken as the datum, and is assumed constant. (In practice, on each occasion that the flow-rate was reduced, the inlet gap also had to be reduced slightly to maintain a constant equilibrium current throughout all the tests. Nevertheless the greatest reduction was only 0·2 mm.) For a gap width increasing along the electrode length, the deviation from the datum is taken as positive. A negative deviation means that the gap width decreases along the electrode (cf. the orientation of the electrodes in Fig. 1).

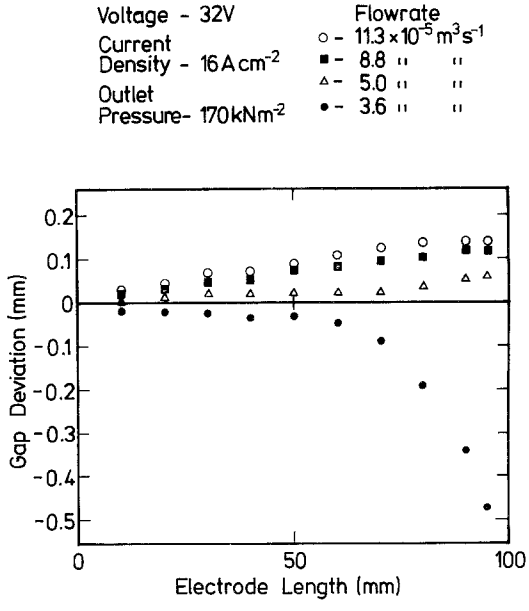

Fig. 4. Influence of electrolyte flow-rate on gap width (NaCl solution).

As the flow-rate is reduced from 11·3 to $5{\cdot}0 \times 10^{-5}$ m^3 s^{-1}, the gap width remains divergent. That is, electrical heating within the gap must have predominated over hydrogen gas evolution in influencing the effective conductivity of the electrolyte solution. At the lowest flow-rate, however, the gap width converges abruptly towards the outlet. These conditions correspond to the occurrence of boiling near the outlet, as shown in Fig. 3. The convergent taper is therefore attributed mainly to the formation of steam bubbles within the gap, which decrease the effective conductivity of the solution, and not simply to the evolution of hydrogen gas bubbles. This result contrasts with those of Hopenfeld and Cole [7], and Thorpe and Zerkle [3], who also report a convergent taper but consider that it is due entirely to hydrogen bubbles which reduce the effective conductivity of the electrolyte.

In a further test series, the voltage was reduced to 16 V and the electrolyte conductivity increased to give an inlet machining gap of 1·60 mm, which is closer to that which is normally encountered in ECM practice, e.g. 0·5 to 1 mm. (The gap was not reduced further to avoid damage to the thermistors.) The other operating conditions shown in Fig. 2 were retained. The trend of results was again similar to those of Fig. 2 except that boiling occurred at a lower flow-rate (about 2×10^{-5} m^3 s^{-1} compared with $3{\cdot}0 \times 10^{-5}$ m^3 s^{-1}), the temperature at outlet for this condition also being lower (about 324 K compared with 340 K). These outlet temperatures also obeyed the predictions from basic Joule heating theory (Equation 1).

Fig. 2 also includes results of tests with 17% (w/w) $NaNO_3$ electrolyte, whose solution has a conductivity similar to that of 10% NaCl electrolyte, although the former evolves considerably less hydrogen gas [10]. For both solutions the temperatures at outlet are similar, as are those recorded within the gap for the highest flow-rates. However, as the flow-rate is reduced, the temperatures within the gap for the nitrate electrolyte become progressively lower than those for the NaCl electrolyte. With much less hydrogen gas produced with the $NaNO_3$ electrolyte, the resistivity of the bubble–electrolyte region, and therefore its resistance heating and temperature, will be correspondingly lower than for the NaCl electrolyte. It has already been suggested that the higher the flow-rate the lower becomes the resistivity of the bubble region of the NaCl solution. Thus at the highest flow-rates the measured temperatures of the two solutions should be closest, and this effect is indicated in Fig. 2.

With the NaCl electrolyte, current efficiency values, based on divalent metal removal, were close to 100% in all tests. However the current efficiency for the $NaNO_3$ solution was found to decrease with decreasing flow-rate to amounts equivalent to virtually complete passivation at the lowest flow-rates (Fig. 5). At these rates, the temperature within the gap is still only slightly greater than that at the outlet (Fig. 2). This result indicates that little hydrogen is evolved for these conditions. The observation is consistent with the work of Mao who reports that little or no hydrogen is evolved

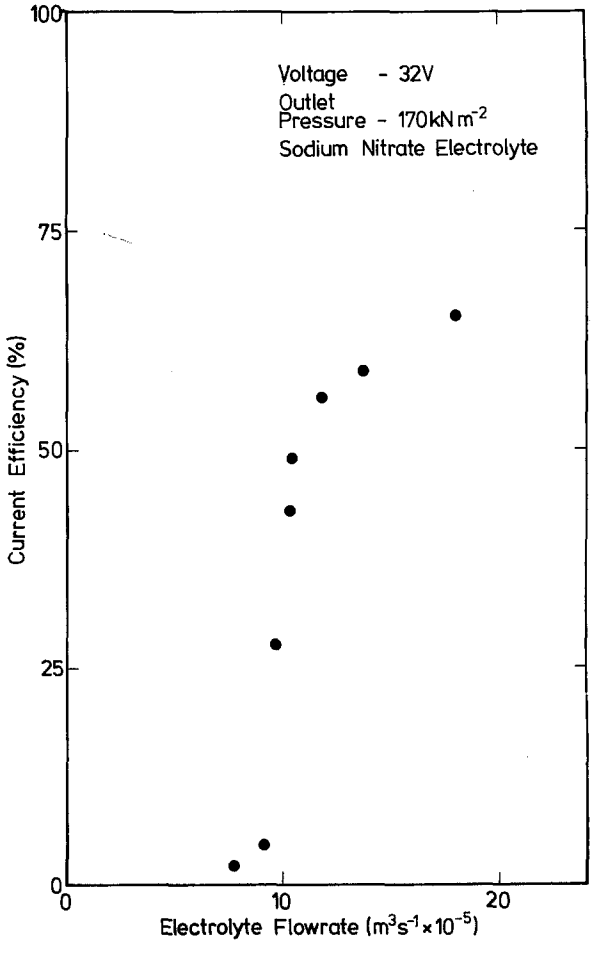

Fig. 5. Effect of electrolyte flow-rate on current efficiency for $NaNO_3$ electrolyte.

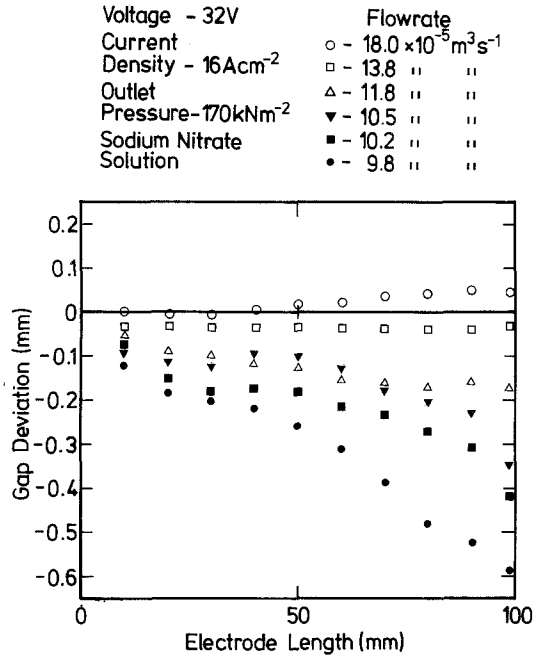

Fig. 6. Influence of electrolyte flow-rate on gap width ($NaNO_3$ solution).

at the cathode when mild steel is machined at low current efficiencies in nitrate solution [10]. For these experimental conditions, the gap width was found to remain constant along the electrode length.

However, for the flow-rates which yield intermediate current efficiencies (e.g. 28% in Fig. 5) the taper in the gap is noted from Fig. 6 to be convergent. Since the volume of hydrogen under these conditions is presumably still small, this effect cannot be attributed to their presence. Instead, it is relevant that Konig and Degenhardt [11] have reported that the current efficiency of steel in nitrate electrolyte decreases as the electrolyte temperature is increased. Since the temperature increase between inlet and outlet for these tests was still substantial – for instance 17 K at a flow-rate of $9{\cdot}8 \times 10^{-5}$ m^3 s^{-1} and at an overall current efficiency of 28% – this temperature increase is suggested to be the main cause of the observed convergent taper. Thus for mild steel machined under such conditions a convergent taper can be caused by a rise in electrolyte temperature even when hydrogen gas bubbles are effectively absent. On that hypothesis an increase in electrolyte flow-rate, by lowering the temperature rise between inlet and outlet, should cause the taper to become less convergent. Again, experimental evidence for this deduction is clear from Fig. 6. Moreover, only when the flow-rate and current efficiency reach their highest values of 18×10^{-5} m^3 s^{-1} and 65% respectively, does the taper become even slightly divergent. At these conditions some hydrogen is evolved. Its presence raises the Ohmic heating within the bubble region with a consequent increase in the effective conductivity of the electrolyte in the downstream direction. Nevertheless, since the amount of hydrogen evolved is still smaller than that with the NaCl electrolyte, the increase in width of the gap along the electrode is still much lower for the $NaNO_3$ solution.

5. Conclusions

(1) The miniature bead-thermistor provides a means of measurement of the temperature of the electrolyte solution within the inter-electrode gap during electrochemical machining.

(2) For NaCl solution, temperatures within the gap can be much higher than those recorded outwith the gap, and can reach the boiling state. This effect can be attributed to measurements carried out in a region of increased resistivity within the gap provided by the hydrogen bubble–electrolyte layer next to the cathode.

(3) For $NaNO_3$ solution, the temperatures within the gap are lower than those found with NaCl electrolyte. This result is consistent with observations that less hydrogen gas is evolved with $NaNO_3$ electrolyte.

Acknowledgements

The authors wish to thank Professor T. M. Charlton for his interest and support and by courtesy of whom the post of research officer has been held by one of them (W. G. C.). The initial stages of this work were carried out at Strathclyde University with the aid of a grant from the Department of Industry and by means of an S. R. C. Research Studentship awarded to W. G. Clark. The authors are grateful to the referee for some useful comments, and to Dr W. M. Ogston and Mr J. R. Thomson for many helpful discussions.

References

[1] See, for example, J. A. McGeough, 'Principles of Electrochemical Machining', Chapter 5, Chapman and Hall, London (1974).

[2] J. W. Cuthbertson and T. S. Turner, *The Production Engineer* **46**, 1 (1967) 1.

[3] J. F. Thorpe and R. D. Zerkle, *Int. J. Mach. Tool Des. Res.* 9 (1969) 131.

[4] International Critical Tables, **3** (1932) 369.

[5] D. Landolt, R. Acosta, R. H. Muller and C. W. Tobias, *J. Electrochem. Soc.* **117** (6) (1969) 839.

[6] A. C. Baxter, H. E. Freer and D. A. Willenbruch, Paper presented at First Int. Conf. on ECM, Leicester University (1973).

[7] J. Hopenfeld and R. R. Cole, *Trans. ASME Series B*, 8 (1969) 755.

[8] A. F. Stronach, J. A. McGeough and W. G. Clark, *Int. J. Mechanical Science* **18** (1976) 261.

[9] S. P. Loutrel and N. H. Cook, *Trans. ASME J. Engineering for Industry*, (1973) 1003.

[10] K. W. Mao, *J. Electrochem. Soc.* **118** (11) (1971) 1876.

[11] W. Konig and H. Degenhardt, 'Fundamentals of Electrochemical Machining', (ed. C. L. Faust), *Electrochem. Soc.* Softbound Symposium Series (1971) 63.